

# Expression of Constitutively Active p21H-ras<sup>Val12</sup> in Postmitotic Pyramidal Neurons Results in Increased Dendritic Size and Complexity

ALÁN ALPÁR,<sup>1\*</sup> KIRSTIN PALM,<sup>1</sup> ANDREAS SCHIERWAGEN,<sup>2</sup> THOMAS ARENDT,<sup>1</sup>  
AND ULRICH GÄRTNER<sup>1</sup>

<sup>1</sup>Department of Neuroanatomy, Paul Flechsig Institut for Brain Research,  
University of Leipzig, D-04109 Leipzig, Germany

<sup>2</sup>Institute for Computer Science, University of Leipzig, D-04109 Leipzig, Germany

---

---

## ABSTRACT

The small G protein p21Ras is a critical molecular switch for relaying neurotrophic actions and is essential for normal functioning and plasticity of the nervous system. In this study, the morphogenetic effects of p21Ras were investigated on neurons *in vivo*. Morphological changes of layers II/III and Vb commissural pyramidal neurons of the primary somatosensory cortex were analyzed in transgenic mice expressing permanently active p21H-Ras<sup>Val12</sup> in postmitotic neurons. Pyramidal cells were retrogradely labelled with biotinylated dextran amine and subsequently traced using NeuroLucida. Compared with wild-type mice, transgenic animals showed a significant increase in the surface area and volume of basal dendrites on the proximal and intermediate segments in layers II/III and on further distal segments in layer V. In addition, the surface area and volume of the trunk and of the proximal segments of oblique branches of apical dendrites were enlarged in both layers. Sholl analyses of basal and apical dendrites showed a significant increase in dendritic complexity of layer V neurons. A positive correlation was observed between the size of the basal dendrite and the neuronal soma size in the transgenic population, indicating that growth-promoting effects of p21H-Ras<sup>Val12</sup> affect both cellular compartments in parallel. However, the dendritic surface correlated with the number of tips and dendritic stem diameter in both wild-type and transgenic populations, demonstrating that these relations represent rather conservative design principles in dendritic morphology. The data presented here suggest an important role of p21Ras-dependent signaling in the final differentiation and maintenance of dendritic morphology. *J. Comp. Neurol.* 467:119–133, 2003. © 2003 Wiley-Liss, Inc.

**Indexing terms:** neurotrophin; small G proteins; cortex; mouse

---

---

Dendritic morphology is the structural correlate for neuronal processing by determination of the number and kinds of inputs a neuron receives. It was long considered that dendrites passively transmit information toward the soma, but recent evidence suggests that dendrites act as dynamic integrators of synaptic input (Hausser et al., 2000). Although dendritic architecture is intrinsically determined to a considerable extent (Bray, 1973; Banker and Cowan, 1979; Bartlett and Banker, 1984), recent studies indicate that dendritic growth is remarkably dynamic and responsive to different environmental signals, including synaptic activity and guidance molecules (McAllister, 2000; Scott and Luo, 2001; Whitford et al., 2002). Signaling from afferents (Rakic, 1975; Miller, 1981; Plaschke et

al., 1995; Wong and Ghosh, 2002) and certain activity patterns (Vaughn, 1989; Kleim et al., 1997) have been

---

Grant sponsor: Deutsche Forschungsgemeinschaft; Grant number: GA 716/1-1; Grant sponsor: Hirnliga e. V.; Grant sponsor: Interdisciplinary Center for Clinical Research at the University of Leipzig; Grant number: IZKF-C1.

\*Correspondence to: Alán Alpár, Paul Flechsig Institute for Brain Research, Department of Neuroanatomy, University of Leipzig, Jahnallee 59, D-04109 Leipzig, Germany. E-mail: dralpar@gmx.net

Received 14 March 2003; Revised 27 May 2003; Accepted 17 July 2003  
DOI 10.1002/cne.10915

Published online the week of October 13, 2003 in Wiley InterScience (www.interscience.wiley.com).

reported to fine tune dendritic growth and patterning, and visual activity has dramatically promoted dendritic arbor growth (Li et al., 2002; Sin et al., 2002). Effects of neurotrophins on cortical neurons have elicited special interest, because they are a prerequisite not only for neuronal development but also for the maintenance of functional stability and plasticity in the adult nervous system (Thoenen, 1995; Davies, 2000; Huang and Reichardt, 2001; McAllister, 2002). Neurotrophins regulate the sprouting as well as the orderly growth and patterning of dendritic trees in both the developing (McAllister et al., 1995, 1996; Baker et al., 1998; Horch et al., 1999; Niblock

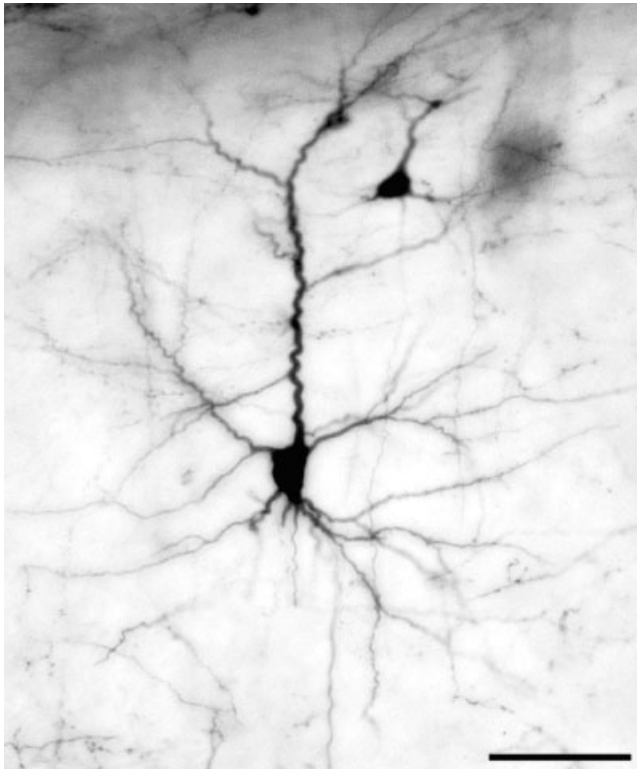


Fig. 1. Light micrograph of a retrogradely labelled (BDA) pyramidal neuron from layers II/III of the transgenic mouse primary somatosensory cortex. Scale bar = 50  $\mu\text{m}$ .

et al., 2000; McAllister, 2002) and the adult (Horch and Katz, 2002) neocortex. They help to establish specific dendritic designs according to certain activity patterns (Horch et al., 1999) by enhancing and opposing effects on dendritic development (McAllister et al., 1997). Finally, neurotrophins have been reported to reverse age-related structural changes (Mervis et al., 1991), to prevent dendritic atrophy (Kolb et al., 1997a), and to stimulate neuronal growth (Kolb et al., 1997b) in the adult nervous system.

Both neuronal activity and neurotrophins guide dendritic development via mechanisms involving GTPase-dependent modulation of the actin cytoskeleton (McAllister, 2000; Li et al., 2002; Sin et al., 2002). Special interest has been focused on the small G proteins of the Rho family. They are known to be powerful intracellular regulators of signaling pathways to the actin cytoskeleton (Luo et al., 1997; Smith, 1999; Meyer and Feldman, 2002) and are, therefore, in a perfect position to mediate neurotrophic or activity-dependent effects on dendritic morphology (McAllister, 2000). Actually, RhoA and also Cdc42 and Rac have been reported to regulate distinct aspects of dendritic arbor growth and remodeling: RhoA prevents dendrite formation and induces dendritic retraction, whereas Rac or Cdc42 activity increases dendritic branch dynamics (Ruchhoeft et al., 1999; Nakayama et al., 2000; Li et al., 2000, 2002; Redmond and Ghosh, 2001; Sin et al., 2002).

Recent studies have drawn attention to the small G protein p21Ras in dendritic growth (Holzer et al., 2001a,b; Huang and Reichardt, 2003). As with other GTPases, p21Ras regulates the phosphorylation of downstream kinases that trigger cascade mechanisms resulting in the regulation of enzymatic activities, ionic channels, cellular morphology, and gene expression (Ahn, 1993; Nishida and Gotoh, 1993; Heumann, 1994). Although p21Ras is a ubiquitous eukaryotic protein, its expression in brain is up

TABLE 1. Somal Perimeter and Somal Areas in Layers II/III and V (Mean  $\pm$  SEM)

	Layers II/III		Layer V	
	Transgenic	Wild-type	Transgenic	Wild-type
Perimeter ( $\mu\text{m}$ )	49.01 $\pm$ 1.82*	38.84 $\pm$ 0.96	53.65 $\pm$ 3.37*	42.21 $\pm$ 1.66
Somal area ( $\mu\text{m}^2$ )	130.18 $\pm$ 5.63*	99.21 $\pm$ 2.76	148.59 $\pm$ 5.64*	98.66 $\pm$ 3.22

\* $P < 0.05$ .

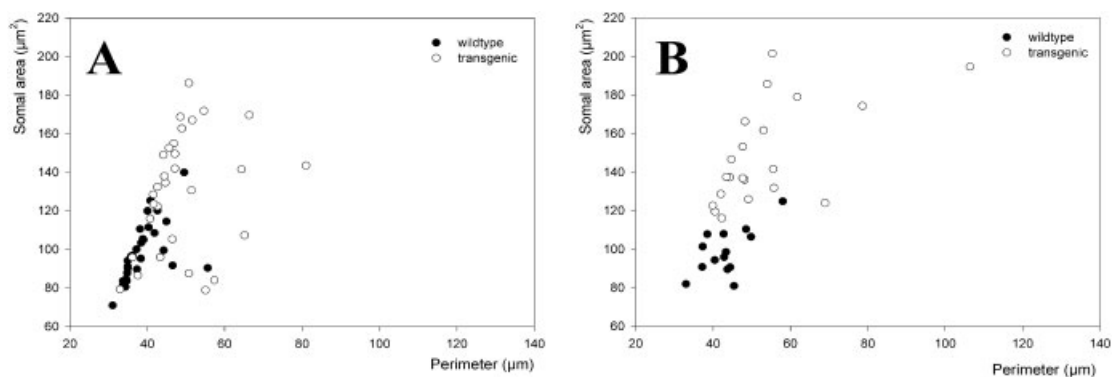


Fig. 2. Effect of transgenic ras on the perimeter and somal area of commissural pyramidal neurons in layers II/III (A) and in layer V (B).

to tenfold higher compared with other tissues (Tanaka et al., 1986; Furth et al., 1987). Pioneering studies have emphasised the crucial role of p21Ras in the differentiation of nerve cells in vitro (Noda et al., 1985; Bar-Sagi and Feramisco, 1985; Guerrero et al., 1986). In the adult nervous system, reactive elevation of p21Ras expression has been demonstrated during dendritic reorganization and compensatory neosynaptogenesis following lesion (Phillips and Belardo, 1994). Furthermore, p21Ras is implicated in the pathology of neurodegenerative diseases, such as Alzheimer's disease (Gärtner et al., 1995, 1999).

The effect of constitutively active p21Ras protein on the mature nervous system has been previously investigated

in p21H-ras<sup>Val12</sup> transgenic mice (Heumann et al., 2000; Holzer et al., 2001a,b). In this transgenic model, the expression of transgenic p21H-Ras<sup>Val12</sup> starts postnatally at about day 15, when neurons are postmitotic and most synaptic contacts have been established. In particular, cortical pyramidal neurons express the transgenic construct at high levels. The volume of the cerebral cortex of these transgenic mice is increased by approximately 20% compared with wild-type mice. This increase has been attributed to the enlarged volume of the cortical pyramidal cells but not to a raise in the number of neurons (Heumann et al., 1996, 2000; Holzer et al., 2001a,b). The aim of the present study was to investigate the effect of

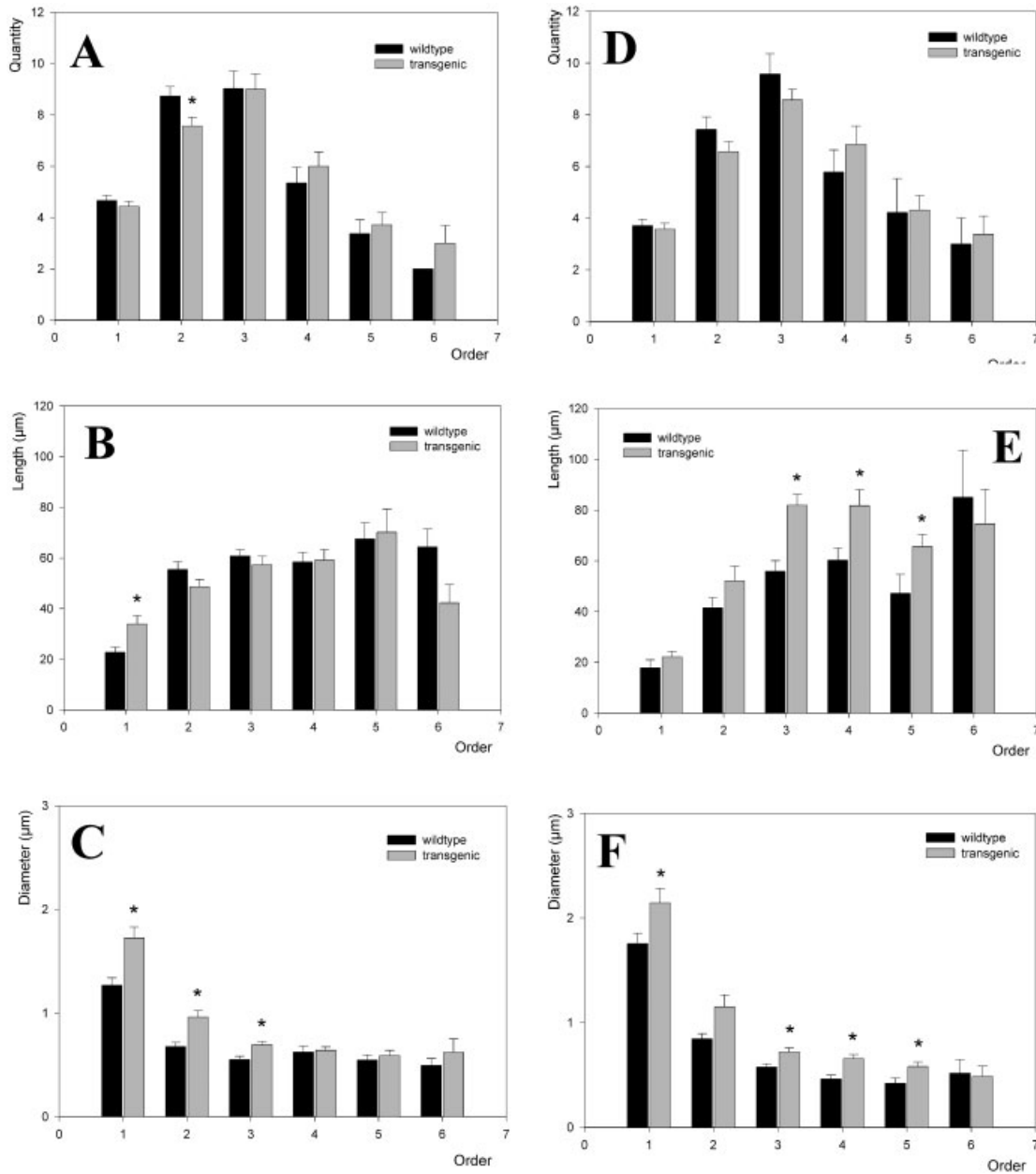


Fig. 3. Comparison between several parameters of basal dendrites in transgenic mice and wild types in layers II/III (A-C) and V (D-F). Bars show the mean values of quantity (A,D), length (B,E), and diameter (C,F) of the basal dendritic orders. Asterisks indicate significant difference between the groups.

TABLE 2. Parameters of Basal Dendrites of Layer II/III Pyramidal Neurons (Mean  $\pm$  SEM)

Order	Quantity		Length ( $\mu\text{m}$ )		Surface area ( $\mu\text{m}^2$ )		Volume ( $\mu\text{m}^3$ )		Diameter ( $\mu\text{m}$ )	
	Transgenic	Wild-type	Transgenic	Wild-type	Transgenic	Wild-type	Transgenic	Wild-type	Transgenic	Wild-type
1	4.43 $\pm$ 0.20	4.67 $\pm$ 0.20	33.90 $\pm$ 3.45*	22.78 $\pm$ 1.99	155.16 $\pm$ 13.63*	79.62 $\pm$ 4.55	73.03 $\pm$ 8.47*	27.49 $\pm$ 2.54	1.73 $\pm$ 0.07*	1.27 $\pm$ 1.72
2	7.57 $\pm$ 0.34*	8.73 $\pm$ 0.36	48.68 $\pm$ 2.90	55.50 $\pm$ 2.99	130.11 $\pm$ 8.33*	104.58 $\pm$ 6.14	33.73 $\pm$ 2.92*	20.14 $\pm$ 2.21	0.96 $\pm$ 0.04*	0.68 $\pm$ 0.96
3	9.00 $\pm$ 0.60	9.03 $\pm$ 0.67	57.33 $\pm$ 3.39	60.80 $\pm$ 2.50	160.57 $\pm$ 31.70*	92.17 $\pm$ 6.91	27.1 $\pm$ 3.61*	15.38 $\pm$ 2.22	0.69 $\pm$ 0.03*	0.55 $\pm$ 0.69
4	6.00 $\pm$ 0.55	5.35 $\pm$ 0.61	59.10 $\pm$ 4.24	58.46 $\pm$ 3.77	109.81 $\pm$ 10.00	90.01 $\pm$ 7.71	19.52 $\pm$ 2.58*	12.53 $\pm$ 1.64	0.64 $\pm$ 0.06	0.63 $\pm$ 0.64
5	3.72 $\pm$ 0.47	3.37 $\pm$ 0.54	70.18 $\pm$ 9.03	67.54 $\pm$ 6.43	121.00 $\pm$ 20.23	91.57 $\pm$ 12.08	18.63 $\pm$ 3.90	11.13 $\pm$ 2.01	0.59 $\pm$ 0.05	0.59 $\pm$ 0.59
6	3.00 $\pm$ 0.68	2.00 $\pm$ 0.00	42.25 $\pm$ 7.21	64.36 $\pm$ 7.08	66.81 $\pm$ 7.56	100.14 $\pm$ 21.67	9.39 $\pm$ 3.43	13.52 $\pm$ 4.67	0.62 $\pm$ 0.07	0.49 $\pm$ 0.62
Total					3,775.34 $\pm$ 271.25*	2,778.91 $\pm$ 140.82	1,000.15 $\pm$ 112.27*	503.57 $\pm$ 41.47		

\* $P < 0.05$ .

constitutively active p21Ras (p21H-Ras<sup>Val12</sup>) on the morphology of pyramidal cells in the neocortex.

The morphology of pyramidal cells is very heterogenous with respect to dendritic variability and complexity (Feldman, 1984). Even within the same region, differences are remarkable: Callosal neurons have been reported to have larger and more complex dendritic arbors for both apical and basal dendritic trees compared with ipsilateral neurons (Soloway et al., 2002). In addition, long corticocortical projection neurons have been shown to establish longer, more complex dendritic arbors than pyramidal neurons projecting locally (Duan et al., 2002). To specify the investigated population of neurons, only commissural pyramidal neurons of the same layers and of the same region were analyzed in the present study.

## MATERIALS AND METHODS

Three 9-month-old B6CBF1  $\times$  NMR1 male transgenic mice carrying a bicistronic construct consisting of p21H-ras<sup>Val12</sup> linked via an internal ribosomal entry site to  $\beta$ -galactosidase cDNA were used. Expression of the transgene is restricted to a subset of neuronal cells by the rat synapsin 1 promoter (described previously by Heumann et al., 1996, 2000). Experiments were carried out on three male wild-type mice as well.

Mice were anesthetized intramuscularly with a cocktail of ketamine (100 mg/kg), xylazine (5 mg/kg), and atropine (0.1 mg/kg) and mounted onto a stereotaxic instrument. Prior to incision, 0.1 ml Xylonest (Astra) was injected below the skin for local anesthesia, the left parietal bone was partially removed, and unilateral injection of biotinylated dextran amine (BDA; 1  $\mu\text{l}$  of 20%, 10,000 MW; Molecular Probes) was delivered mechanically with a Hamilton syringe into the corpus callosum 1 mm lateral to the midline and 0.5 mm caudal to the bregma, 1 mm deep from the pial surface according to the stereotaxic atlas of Franklin and Paxinos (1997). Seven days later, the animals were intracardially perfused while under deep anesthesia, first with saline (0.9% NaCl) for 1–2 minutes and then with a fixative containing 4% paraformaldehyde in 0.1 M phosphate buffer (pH 7.4) for 30 minutes. The brains were postfixed in the same fixative overnight, immersed in 30% sucrose for another 24 hours, and sectioned (160  $\mu\text{m}$ ) in the coronal plane on a cryostat. The free-floating sections were extensively washed in 0.05 M Tris-buffered saline (TBS; pH 7.4) and then reacted with the avidin-biotin-peroxidase complex (1:100 in TBS; Vectastain Elite ABC Kit; Vector Laboratories, Burlingame, CA) at room temperature for 2 hours. BDA was visualised by using 3,3'-diaminobenzidine (0.025%; Sigma, St. Louis, MO) intensified with nickel-ammonium sulfate (0.05%; Merck, Darmstadt, Germany) in the presence of 0.001% hydrogen peroxide diluted in TBS. Sections were mounted onto gelatin-coated glass slides, dehydrated, and covered with DPX (Fluka, Heidelberg, Germany).

The retrogradely labelled commissural pyramidal cells in the primary somatosensory cortex were traced using NeuroLucida (MicroBrightField, Inc., Colchester, VT). Briefly, the perikaryal outline and the route of the dendrite were followed on the monitor screen by using a computer mouse, and the mouse wheel allowed continuous adjustment of the dendritic diameter. A motorized stage with position encoders allowed navigation through the section in the X, Y, and Z axes and the accurate acquisition of the spatial coordinates of the measured structure. All

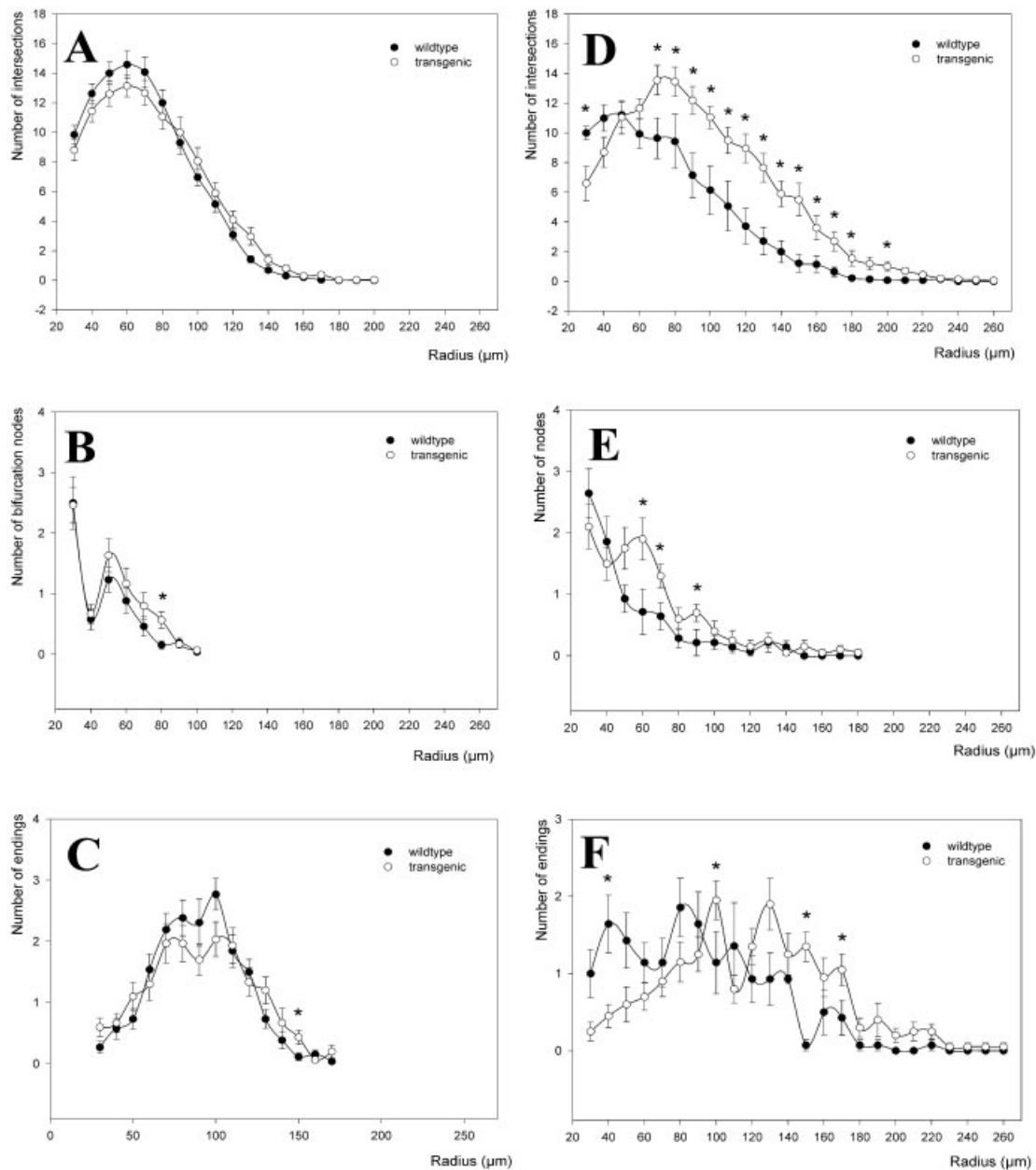


Fig. 4. Sholl analysis of basal dendritic tree in layers II/III (A–C) and V (D–F). Numbers of dendritic intersections (A), bifurcation nodes (10- $\mu$ m bin; B), and tips (C) show similar rising and falling phases in layers II/III; significant differences are seen in layer V (D–F). Asterisks indicate significant difference between the groups.

visible dendrites were traced without marking eventual truncation of smaller dendritic sections. This might have led to a certain underestimation of the dendritic tree, especially in transgenic mice with a larger dendritic arbor. To gain both sufficient transparency for optimal tracing and at the same time a neuronal reconstruction as complete as possible, sections of 160  $\mu$ m thickness were used. Thicker sections allowed only ambiguous tracing of thinner dendritic branches. Shrinkage correction (300%) was carried out in the Z axis, but not in the X,Y plane, because shrinkage was negligible in these dimensions ( $\sim$ 10%). The three-dimensional (3D) reconstructions of traced neurons

were analyzed with NeuroExplorer (MicroBrightField, Inc.). The following data were calculated and used for further analysis: 1) cell body: perimeter and surface area (two-dimensional projection); 2) basal dendrites: quantity; number of branches and tips; length, diameter, surface area, and volume (total and mean) per neuron and per dendritic order; 3) apical dendrite: number of branches and tips; length, diameter, surface area, and volume (total and mean) per neuron; the same data for shaft, orders of oblique dendrites and terminal arbor were also gained; 4) Sholl analysis of basal and apical dendrites: number of intersections, tips, and bifurcation nodes (branching

TABLE 3. Parameters of Basal Dendrites of Layer V Pyramidal Neurons (Mean  $\pm$  SEM)

Order	Quantity		Length ( $\mu\text{m}$ )		Surface area ( $\mu\text{m}^2$ )		Volume ( $\mu\text{m}^3$ )		Diameter ( $\mu\text{m}$ )	
	Transgenic	Wild-type	Transgenic	Wild-type	Transgenic	Wild-type	Transgenic	Wild-type	Transgenic	Wild-type
1	3.57 $\pm$ 0.22	3.71 $\pm$ 0.24	22.17 $\pm$ 2.20	17.94 $\pm$ 3.05	134.72 $\pm$ 12.43*	93.95 $\pm$ 17.57	76.37 $\pm$ 8.67*	42.02 $\pm$ 8.87	2.15 $\pm$ 0.14*	1.76 $\pm$ 0.09
2	6.57 $\pm$ 0.39	7.43 $\pm$ 0.49	52.21 $\pm$ 5.79	41.52 $\pm$ 4.13	154.88 $\pm$ 12.99*	93.21 $\pm$ 10.21	49.11 $\pm$ 6.12*	22.68 $\pm$ 3.05	1.15 $\pm$ 0.11	0.85 $\pm$ 0.05
3	8.57 $\pm$ 0.41	9.57 $\pm$ 0.79	81.95 $\pm$ 4.37*	55.86 $\pm$ 4.18	166.22 $\pm$ 9.97*	90.88 $\pm$ 7.19	27.19 $\pm$ 3.80*	15.06 $\pm$ 1.78	0.72 $\pm$ 0.04*	0.58 $\pm$ 0.03
4	6.86 $\pm$ 0.71	5.79 $\pm$ 0.85	81.79 $\pm$ 6.21*	60.28 $\pm$ 4.81	155.99 $\pm$ 10.51*	84.05 $\pm$ 9.07	29.41 $\pm$ 2.88*	10.96 $\pm$ 1.63	0.66 $\pm$ 0.04*	0.46 $\pm$ 0.03
5	4.32 $\pm$ 0.56	4.22 $\pm$ 1.31	65.65 $\pm$ 4.80*	47.26 $\pm$ 7.44	101.12 $\pm$ 9.94*	65.38 $\pm$ 13.84	17.37 $\pm$ 2.56*	8.37 $\pm$ 2.22	0.58 $\pm$ 0.05*	0.42 $\pm$ 0.05
6	3.38 $\pm$ 0.71	3.00 $\pm$ 1.00	74.67 $\pm$ 13.58	85.05 $\pm$ 18.62	17.72 $\pm$ 9.63	23.44 $\pm$ 10.43	10.57 $\pm$ 9.63	23.44 $\pm$ 10.43	0.49 $\pm$ 0.09	0.52 $\pm$ 0.13
Total					4,961.6 $\pm$ 363.48*	2,790.83 $\pm$ 402.10	1,250.21 $\pm$ 147.69*	594.74 $\pm$ 95.55		

\* $P < 0.05$ .

points). Statistical analysis of morphological measures was performed using a multifactorial ANOVA, with strain (wild-type vs. transgenic) as the between-groups factor and radius or branch order as the within-subjects factors. Student's  $t$ -tests was used in the post hoc analysis. Correlative analyses were carried out using linear regression. The significance level was set at  $P < .05$ , and computations were performed using the Prophet 5.0 statistical package. The photomicrograph (Fig. 1) was taken with a digital microscope camera AxioCam HRC running on AxioVision 3.1 software (both from Carl Zeiss Vision) and were adjusted in Corel Draw 8.0.

## RESULTS

The injections applied into the corpus callosum resulted in retrograde labelling of many neurons within layers II, III, and Vb of the motor and sensory cortices of both hemispheres. Anterogradely labelled commissural fibers and terminals were also found in the same regions throughout all layers of the cortex. Pyramidal neurons in the primary somatosensory cortex were selected for further analysis. In layers II/III, 30 neurons were traced in transgenic and another 30 neurons in wild-type mice. In layer Vb, 21 neurons were traced in transgenic and 14 in wild-type mice. A typical BDA-labelled neuron is shown in Figure 1.

### Cell body

No detailed investigations were carried out on the soma. By using the NeuroLucida system, the area and perimeter of the two-dimensional projection of the soma were calculated. Both parameters as measured in layers II/III and V, respectively, are significantly larger in transgenic compared with wild-type mice (Table 1). In both layers, perikarya with equivalent perimeters have larger somal areas in the transgenic animals (Fig. 2A,B).

### Basal dendrites

**Main observations.** In both layers, the surface area and volume of the basal dendritic tree in the p21H-Ras<sup>Val12</sup> transgenic mice are considerably larger than in the wild type (see Fig. 7A,B). This is determined mainly from increased dendritic diameter but also from segment elongation in layer V. The dendritic density of layer V neurons is significantly higher in transgenic mice.

**Layers III/II.** There is no global difference in the number of segments per order between wild-type and transgenic populations (Fig. 3A). However, additional dendritic orders appear in the transgenic neurons. Seventh-order segments were found in seven transgenic neurons but only in one wild-type cell, and eighth-order segments were found only in two transgenic cells. First-order segments of transgenic cells are elongated (Fig. 3B). The average diameters of the first three dendritic orders are increased (Fig. 3C) as well as the resulting surface area and volume (Table 2). In total, the size of the basal dendritic tree is dramatically enlarged (see Fig. 7A,B). Curves of Sholl analyses are very similar for both populations (Fig. 4A–C). The number of bifurcation nodes reaches its maximum at 30  $\mu\text{m}$  and at 50  $\mu\text{m}$ , which leads to a peak in the number of dendritic intersections at 60  $\mu\text{m}$ .

**Layer V.** Although there are no differences in the number of segments (Fig. 3D), the mean length of inter-

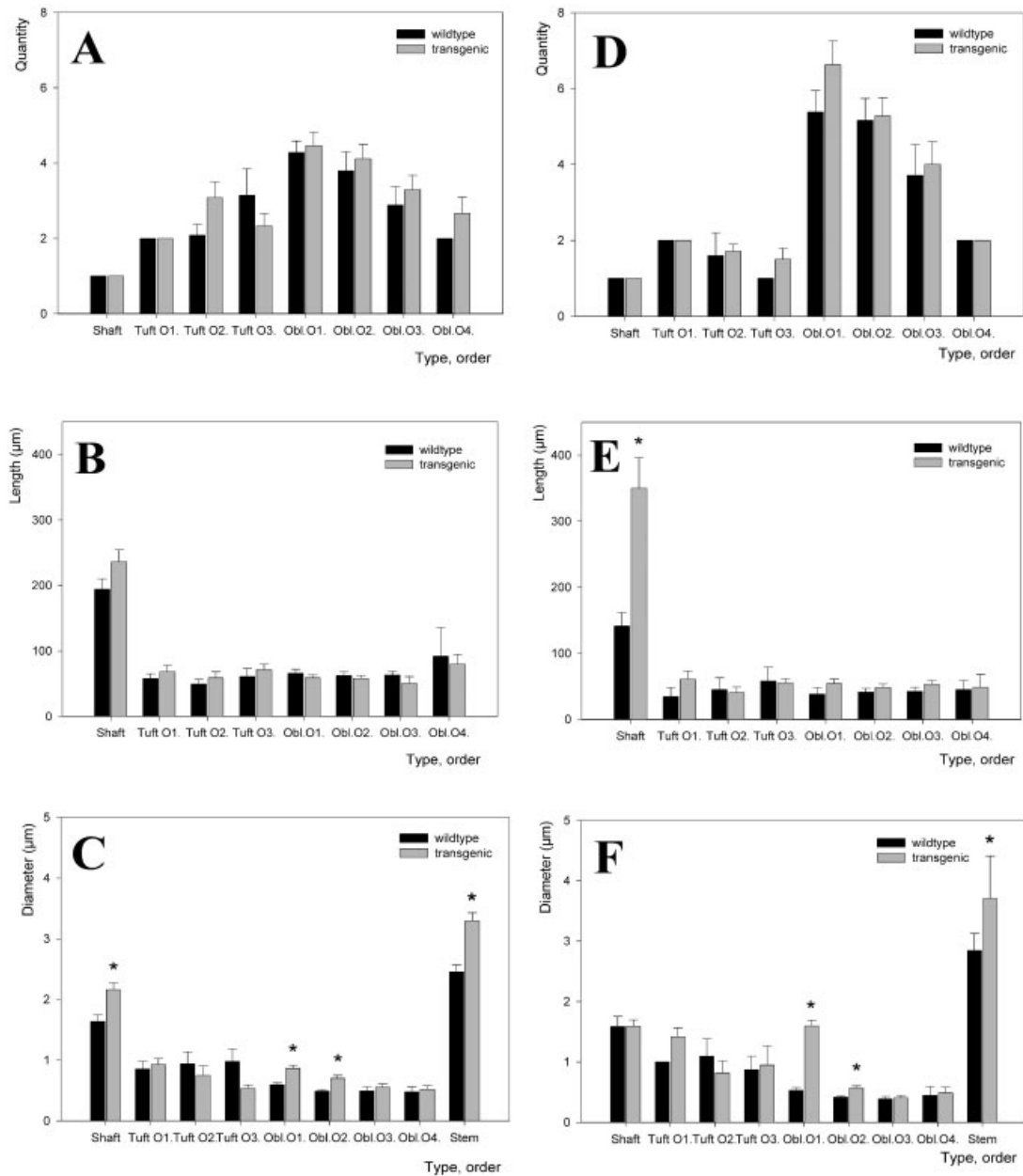


Fig. 5. Comparison between several parameters of apical dendrites in transgenic mice and wild types in layers II/III (A-C) and V (D-F). Bars show the mean values of quantity (A,D), length (B,E), and diameter (C,F) of different parts and orders of the apical dendritic tree. Asterisks indicate significant difference between the groups.

mediate segments (orders 3–5) is extended (Fig. 3E), and the average diameters of most dendritic orders are enlarged in transgenic mice (Fig. 3F). Corresponding to the increased diameters and lengths of segments, their surface area and volume are augmented as well (Table 3), resulting finally in the significant enlargement of the whole basal dendritic tree (see Fig. 7A,B). Similarly to layer II/III pyramidal cells, there are additional dendritic orders in the transgenic cell population. Seventh-order dendrites were found in two cells of the wild-type group but in six cases of the transgenic group, eighth (3 cases)- and ninth (2 cases)-order segments were found only

among the transgenic population. In contrast to the case for layer II/III neurons, Sholl analysis reveals significant differences between transgenic and wild-type populations (Fig. 4D–F). The course of the intersection curve is similar in both types (Fig. 4D). In the wild type, the peak of dendritic density occurs between 30 μm and 50 μm. In contrast, the maximum of dendritic intersections of transgenic cells is higher and is shifted toward a greater distance (between 70 μm and 80 μm) from the soma. Accordingly, in transgenic cells, the number of intersections is higher at radii over 60 μm (Fig. 4D). The number of branching points is elevated at several radii in the trans-

TABLE 4. Parameters of Apical Dendrites of Layer II/III Pyramidal Neurons (Mean  $\pm$  SEM)

	Quantity		Length ( $\mu\text{m}$ )		Surface area ( $\mu\text{m}^2$ )		Volume ( $\mu\text{m}^3$ )		Diameter ( $\mu\text{m}$ )	
	Transgenic	Wild-type	Transgenic	Wild-type	Transgenic	Wild-type	Transgenic	Wild-type	Transgenic	Wild-type
Shaft	1.00 $\pm$ 0.00	1.00 $\pm$ 0.00	236.15 $\pm$ 18.4	194.16 $\pm$ 15.97	1,426.6 $\pm$ 96.53*	842.43 $\pm$ 44.88	826.77 $\pm$ 76.51*	360.69 $\pm$ 25.91	2.16 $\pm$ 0.11*	1.64 $\pm$ 0.11
Tuft I	2.00 $\pm$ 0.00	2.00 $\pm$ 0.00	68.39 $\pm$ 9.46	57.95 $\pm$ 7.34	172.56 $\pm$ 23.4	121.15 $\pm$ 13.45	44.77 $\pm$ 8.88	27.97 $\pm$ 5.17	0.93 $\pm$ 0.09	0.86 $\pm$ 0.13
Tuft II	3.08 $\pm$ 0.41	2.08 $\pm$ 0.28	59.00 $\pm$ 8.25	49.43 $\pm$ 7.10	131.07 $\pm$ 33.48	141.89 $\pm$ 53.29	31.66 $\pm$ 12.02	53.79 $\pm$ 35.06	0.75 $\pm$ 0.15	0.94 $\pm$ 0.19
Tuft III	2.33 $\pm$ 0.33	3.14 $\pm$ 0.70	71.35 $\pm$ 8.56	60.71 $\pm$ 12.31	122.40 $\pm$ 23.85	179.89 $\pm$ 56.31	15.99 $\pm$ 4.86	57.79 $\pm$ 27.04	0.54 $\pm$ 0.06	0.98 $\pm$ 0.21
ObI. I	4.47 $\pm$ 0.36	4.29 $\pm$ 0.50	58.76 $\pm$ 4.55	66.07 $\pm$ 6.02	147.12 $\pm$ 12.70*	112.58 $\pm$ 8.39	36.45 $\pm$ 4.85*	17.76 $\pm$ 1.63	0.87 $\pm$ 0.05*	0.59 $\pm$ 0.03
ObI. II	4.12 $\pm$ 0.39	3.79 $\pm$ 0.50	57.99 $\pm$ 4.16	62.47 $\pm$ 5.53	120.28 $\pm$ 11.31	94.63 $\pm$ 9.68	23.96 $\pm$ 3.47*	12.89 $\pm$ 1.78	0.70 $\pm$ 0.05*	0.49 $\pm$ 0.03
ObI. III	3.29 $\pm$ 0.38	2.89 $\pm$ 0.48	50.6 $\pm$ 10.26	63.30 $\pm$ 5.43	105.53 $\pm$ 28.79	97.95 $\pm$ 17.53	18.91 $\pm$ 7.49	14.49 $\pm$ 4.77	0.56 $\pm$ 0.05	0.49 $\pm$ 0.07
ObI. IV	2.67 $\pm$ 0.42	2.00 $\pm$ 0.00	79.85 $\pm$ 14.83	92.00 $\pm$ 43.58	122.22 $\pm$ 19.14	157.61 $\pm$ 100.90	17.08 $\pm$ 3.14	23.69 $\pm$ 17.99	0.52 $\pm$ 0.06	0.48 $\pm$ 0.09
Total					3,397.39 $\pm$ 240.43*	2,515.75 $\pm$ 218.81	1,298.9 $\pm$ 125.50*	657.72 $\pm$ 82.01		

\* $P < 0.05$ .

genic population beyond 50  $\mu\text{m}$  (Fig. 4E), such as the number of tips beyond 100  $\mu\text{m}$  (Fig. 4F).

### Apical dendrite

**Main observations.** In both layers, the surface area and volume of the apical tree are considerably larger in transgenic compared with wild-type mice (see Fig. 7A,B). These changes are caused principally by increased dendritic segment caliber. In layer V, the dendritic tree is more arborized.

**Layers II/III.** The majority of pyramidal neurons carried one apical trunk, which bifurcated into two primary-order segments in the terminal arbor. Pyramidal neurons with two apical dendrites were not considered in the analysis. There is no difference in the number and length of dendritic segments between the groups (Fig. 5A,B). The apical trunk and the first two orders of the oblique dendrites are characterized by enlarged average diameter, surface area, and volume in transgenic mice (Table 4, Fig. 5C). Sholl analysis reveals no differences in any of the considered parameters (number of intersections, bifurcation nodes and tips; Fig. 6A–C). The maximum of dendritic intersections is located between 70  $\mu\text{m}$  and 80  $\mu\text{m}$  in both populations (Fig. 6A). The distance of branching points of oblique dendrites from soma was also analyzed; however, no differences were found between transgenic and wild-type neurons (see Table 6).

**Layer V.** The number and the length of dendritic segments were not changed in the transgenic population; however, the apical trunk was considerably elongated (Fig. 5D,E). The stem diameter of the apical trunk and the average diameter of the first two orders of oblique dendrites were enlarged in the transgenic mice (Table 5, Fig. 5F). Accordingly, surface area and volume of these segments were enlarged (Table 5). Sholl analysis revealed a global increase of dendritic intersections in the transgenic population (Fig. 6D), but the maximum occurred at the same distance from the soma as in the wild type (between 60  $\mu\text{m}$  and 80  $\mu\text{m}$ ). No differences were found in the number and distribution of bifurcation nodes or tips (Fig. 6E,F). Oblique dendrites branch from the apical trunk at very similar distances from soma in both groups (Table 6).

### Correlations

Previous studies have demonstrated that several parameters of neuronal morphology do not vary independently from each other. Such interrelations between parameters might help to uncover principal design rules of dendritic geometry that are characteristic of distinct neuron types (Larkman, 1991a,b). To specify further the effects of transgenic p21Ras on dendritic morphology, parameters representing the dendritic size were correlated with characteristic neuronal measures, such as somal size, dendritic stem diameter, and number of tips.

**Whole-cell correlations.** In both layers, the total volume of basal dendrites correlates positively with the soma size in the transgenic group, but not in the wild type (Fig. 8A,B). On the contrary, the volume of apical dendrite correlates positively with soma size in wild-type but not in transgenic animals (Fig. 8C,D).

**Stem diameter correlations.** The surface area (Fig. 9A,B) and volume of the basal dendritic trees of layers II/III as well as of layer V neurons display a positive correlation with the stem segment diameter in both groups of animals. However, in the transgenic population of layer V neurons, this correlation is shifted so that the



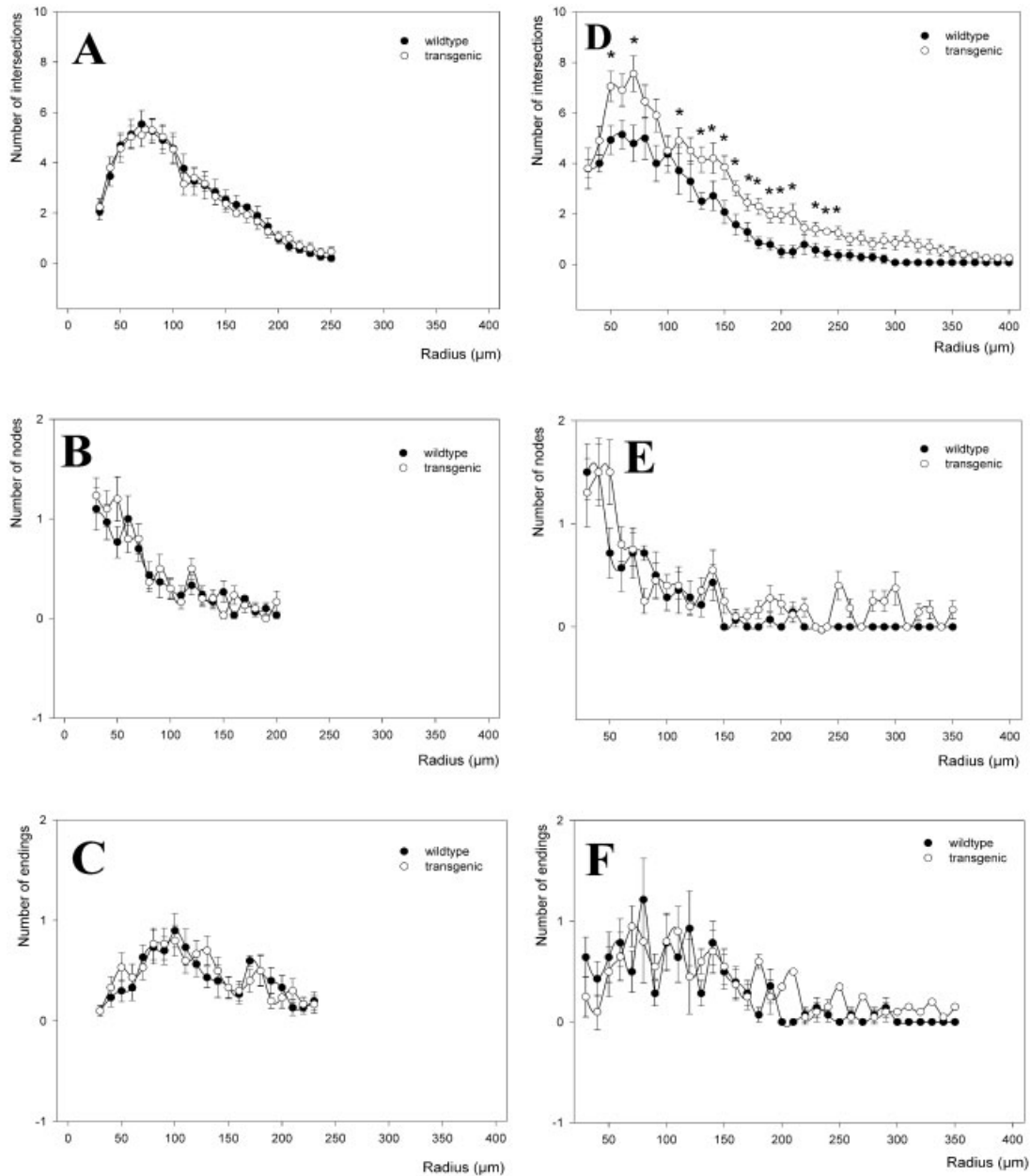


Fig. 6. Sholl analysis of the apical dendritic tree in layers II/III (A-C) and V (D-F). Numbers of bifurcation nodes (B,E) and tips (C,F) show similar very similar values in both layers. Number of intersections increased significantly in layer V (D) but not in layers II/III (A). Asterisks indicate significant difference between the groups.

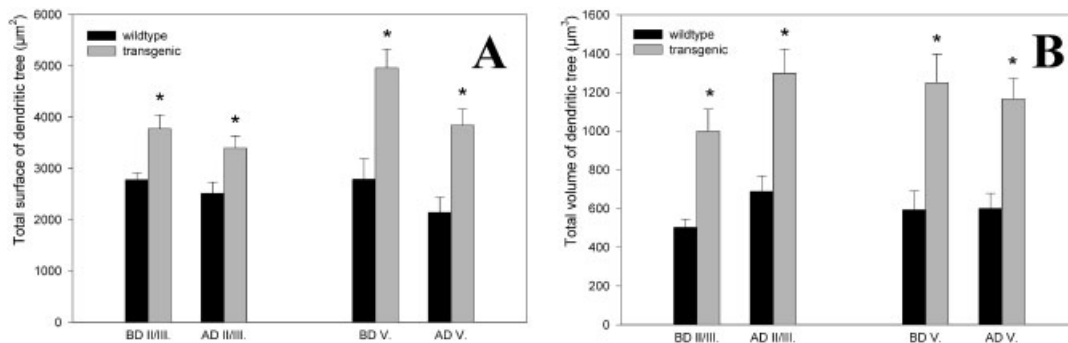


Fig. 7. Total surface area (A) and total volume (B) of basal and apical dendrites are considerably enlarged in transgenic mice compared with wild types. Asterisks indicate significant difference between the groups. BD, basal dendrite; AD, apical dendrite; II/III, layers II/III; V, layer V.

TABLE 5. Parameters of Apical Dendrites of Layer V Pyramidal Neurons (Mean  $\pm$  SEM)

	Quantity		Length ( $\mu\text{m}$ )		Surface area ( $\mu\text{m}^2$ )		Volume ( $\mu\text{m}^3$ )		Diameter ( $\mu\text{m}$ )	
	Transgenic	Wild-type	Transgenic	Wild-type	Transgenic	Wild-type	Transgenic	Wild-type	Transgenic	Wild-type
Shaft	1.00 $\pm$ 0.00	1.00 $\pm$ 0.00	349.88 $\pm$ 46.43*	141.39 $\pm$ 20.48	1,390.10 $\pm$ 177.56*	588.13 $\pm$ 72.08	615.34 $\pm$ 79.12*	248.95 $\pm$ 36.53	1.59 $\pm$ 0.10	1.59 $\pm$ 0.16
Tuft I	2.00 $\pm$ 0.00	2.00 $\pm$ 0.00	60.73 $\pm$ 12.74	34.69 $\pm$ 13.71	99.47 $\pm$ 19.04	64.97 $\pm$ 12.25	18.19 $\pm$ 4.45	15.03 $\pm$ 1.94	1.42 $\pm$ 0.15	1.00 $\pm$ 0.00
Tuft II	1.7 $\pm$ 0.18	1.60 $\pm$ 0.60	40.54 $\pm$ 8.50	45.11 $\pm$ 7.89	108.94 $\pm$ 31.28	98.29 $\pm$ 34.84	30.21 $\pm$ 10.49	22.74 $\pm$ 11.59	0.83 $\pm$ 0.19	1.09 $\pm$ 0.23
Tuft III	1.50 $\pm$ 0.29	1.00 $\pm$ 0.00	55.4 $\pm$ 6.20	58.18 $\pm$ 21.02	156.64 $\pm$ 56.56*	132.40 $\pm$ 34.76	45.08 $\pm$ 22.16*	30.51 $\pm$ 9.24	0.95 $\pm$ 0.32	0.87 $\pm$ 0.29
ObI. I	6.63 $\pm$ 0.62	5.38 $\pm$ 0.56	54.26 $\pm$ 6.79	38.29 $\pm$ 9.85	88.53 $\pm$ 6.79*	57.60 $\pm$ 9.85	25.82 $\pm$ 11.9*	8.91 $\pm$ 1.89	1.59 $\pm$ 0.09*	0.53 $\pm$ 0.05
ObI. II	5.28 $\pm$ 0.48	5.17 $\pm$ 0.58	48.44 $\pm$ 4.99	41.49 $\pm$ 5.07	79.46 $\pm$ 8.57	51.63 $\pm$ 7.57	12.19 $\pm$ 1.52	6.05 $\pm$ 1.17	0.57 $\pm$ 0.03*	0.42 $\pm$ 0.03
ObI. III	4.00 $\pm$ 0.59	3.71 $\pm$ 0.80	53.35 $\pm$ 5.12	42.31 $\pm$ 6.39	65.68 $\pm$ 8.85	52.08 $\pm$ 10.27	7.66 $\pm$ 1.41	5.61 $\pm$ 1.43	0.41 $\pm$ 0.04	0.39 $\pm$ 0.04
ObI. IV	2.00 $\pm$ 0.00	2.00 $\pm$ 0.00	48.85 $\pm$ 19.46	45.51 $\pm$ 3.60	82.36 $\pm$ 33.59	55.51 $\pm$ 4.11	11.76 $\pm$ 4.89	6.45 $\pm$ 2.48	0.49 $\pm$ 0.09	0.44 $\pm$ 0.15
Total					3,844.99 $\pm$ 312.49*	2,143.45 $\pm$ 293.18	1,166.58 $\pm$ 105.56*	601.42 $\pm$ 77.85		

\* $P < 0.05$ .

surface of dendritic trees is larger compared with that of the wild type at equivalent stem diameters (Fig. 9B). The size of apical arbors of layer II/III neurons is similarly related to the stem diameter in both groups (Fig. 9C), whereas the surface area of apical dendrites in layer V is rather independent of the stem diameter (Fig. 9D).

**Tip number correlations.** In both cortical layers, the surface area of basal and apical dendrites is highly correlated with the number of tips. Plots illustrate that dendrites with an equivalent number of endings have a larger surface area in the transgenic group (Fig. 10A–D).

## DISCUSSION

The small G protein p21Ras, which is crucially involved in neurotrophic signal transduction pathways, has been implicated as being essential for normal functioning and plasticity of both the developing (Noda et al., 1985; Barsagi and Feramisco, 1985; Guerrero et al., 1986) and the adult (Brambilla et al., 1997; Silva et al., 1997; Moore et al., 2000) nervous system. Furthermore, enhanced expression of p21Ras is associated with neuronal restructuring after lesion or in the context of neurodegenerative diseases (Phillips and Belardo, 1994; Gärtner et al., 1995, 1999). In the present study, the effect of permanently active p21Ras on the morphology of pyramidal neurons was investigated when main developmental changes were already completed. We took advantage of a transgenic mouse line, in which p21H-Ras<sup>Val12</sup> is postnatally expressed starting at about day 15, when neurons are postmitotic (Heumann et al., 2000).

Because dendritic morphology of pyramidal cells is very heterogeneous, not only in different areas (Jacobs et al., 1997, 2001; Elston and Rockland, 2002) but also within the same region (Duan et al., 2002; Soloway et al., 2002), the investigated population of cells was confined to commissural neurons of layers II/III and V of the primary somatosensory cortex. Although this restriction means a limitation of the present study, it allowed an analysis of a relatively homogeneous subpopulation of pyramidal neurons.

The most obvious alteration of pyramidal cells in the transgenic cortex is an increased somal and dendritic size. In both layers, the somal area and perimeter are larger in transgenic mice. Nothing conspicuous concerning the perikaryal contour was noticed in the transgenic group. However, the fact that somal areas even at equivalent somal perimeters were greater in transgenic than in wild-type mice might be a sign of specific changes in the geometrical proportions of perikarya that could not be specified in detail. Changes in dendritic size were analyzed comprehensively. In both layers, surface area and volume of proximal and intermediate dendritic segments were significantly augmented. This was true also for more distal segments in layer V, where differences were more pronounced. No significant changes were seen in the number of dendritic segments; however, in some cases, additional orders were observed. Surface and volumetric changes resulted mainly from increased dendritic caliber and in layer V also from segment elongation. Consequently, the total surface area and the total volume of dendritic trees were greatly increased. Considering that pyramidal neurons are the numerically dominant cell type of the neocortex (Braitenberg, 1978) and that their dendrites occupy much of the brain's volume (Ramón y Cajal, 1955), we suggest that the increase in somal and dendritic

size is large enough to account for the increased cortical volume described previously (Heumann et al., 2000).

Series of Sholl analyses shed light on differences in the dendritic complexity of layer V neurons. Basal dendrites established more bifurcation nodes in transgenic mice, which led to an increase in dendritic density in intermediate and distal regions of the dendritic tree. Similar alterations were observed in the apical arbor.

The present data clearly indicate that an enhanced p21Ras activity results in a dramatically enlarged and more complex dendritic tree. Previous authors have reported that differences in the size of dendritic receptive surface were parallel to changes observed in the number of synapses (Müller et al., 1984) and that a clear positive relationship exists between spine density and dendritic

diameter (Feldman, 1975; Feldman and Dowd, 1975). The vast majority of excitatory synapses to cortical pyramidal cells was established on spines (Colonnier, 1968), with a proportion that has been estimated to be as high as 95% (Diamond et al., 1970). Therefore, the possibility of further synapse formation evidently grows in transgenic mice, on both dendritic shafts and spines. Actually, the number of synapses in layers II/III has been reported to be increased in this transgenic mouse line. These morphological changes might influence the effectiveness of signal processing.

Because at least some aspects of neuronal morphology follow specific design rules that are represented by the interrelation of morphometric parameters (Larkman, 1991b), further analyses addressed the question of

TABLE 6. Distance of Branching Points of Oblique Dendrites in Layers II/III and V (Mean ± SEM)

Oblique branch	Layers II/III		Layer V	
	Transgenic	Wild-type	Transgenic	Wild-type
1	28.71 ± 25.02	27.76 ± 18.20	11.56 ± 5.79	12.86 ± 3.99
2	60.49 ± 33.10	63.07 ± 38.93	26.61 ± 15.82	24.86 ± 12.05
3	108.14 ± 68.60	105.31 ± 65.18	46.64 ± 42.10	46.36 ± 32.37
4	157.89 ± 105.74	148.36 ± 80.95	87.08 ± 83.75	82.29 ± 47.58
5	159.29 ± 63.89	169.27 ± 89.33	104.15 ± 66.37	117.44 ± 55.30
6	207.75 ± 66.43	165.17 ± 81.56	172.22 ± 82.53	131.03 ± 70.10
7	247.46 ± 91.87	209.13 ± 70.63	211.70 ± 109.65	128.03 ± 47.31
8			264.99 ± 137.87	136.1 ± 69.97
9			222.16 ± 46.37	161.05 ± 8.98

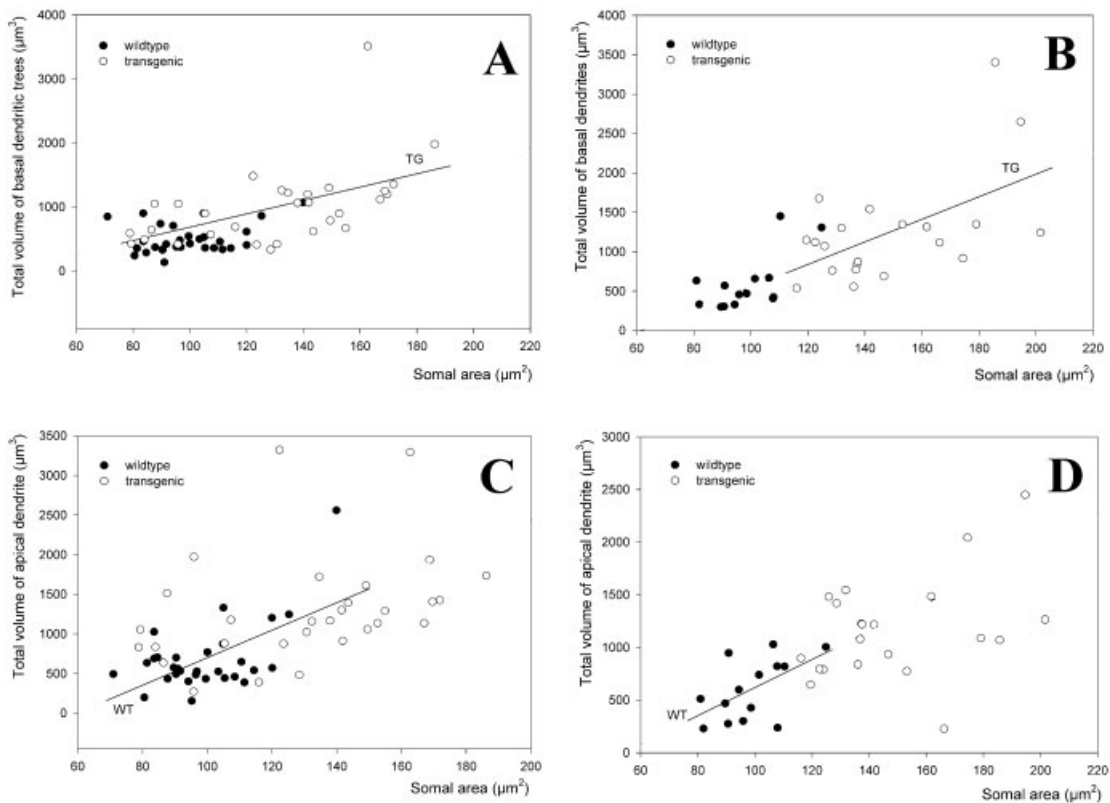


Fig. 8. Correlations between somal area and total volume of dendrites. **A:** Total volume of basal dendritic tree in layers II/III (TG:  $r = 0.52$ ,  $P = 0.003$ ). **B:** Total volume of basal dendritic tree in layer V (TG:  $r = 0.54$ ,  $P = 0.01$ ). **C:** Total volume of apical dendrite in layers II/III (WT:  $r = 0.58$ ,  $P = 0.0007$ ). **D:** Total volume of apical dendrite in layer V (WT:  $r = 0.55$ ,  $P = 0.04$ ).

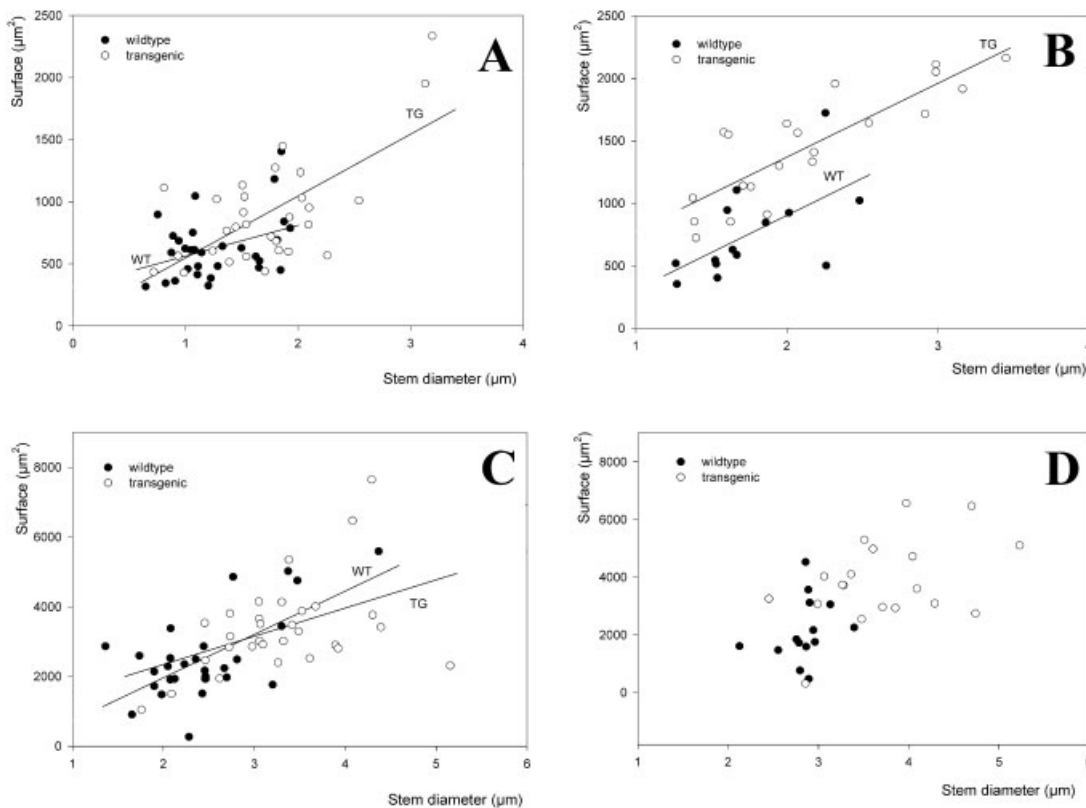


Fig. 9. Correlations between diameter of dendritic stem segments and dendritic surface area. **A:** Layers II/III, basal dendrites (TG:  $r = 0.66$ ,  $P < 0.0001$ ; WT:  $r = 0.38$ ,  $P = 0.04$ ). **B:** Layer V, basal dendrites (TG:  $r = 0.85$ ,  $P < 0.0001$ ; WT:  $r = 0.6$ ,  $P = 0.02$ ). **C:** Layers II/III, apical dendrites (TG:  $r = 0.45$ ,  $P = 0.01$ ; WT:  $r = 0.64$ ,  $P = 0.0002$ ). **D:** Layer V, apical dendrites.

whether such correlations might be altered in the transgenic population. In both layers, the positive correlation between somal size and apical dendritic volume found in the wild type could not be verified in transgenic mice. On the other hand, in contrast to the case in the wild type, the soma size is highly correlated with both surface area and volume of basal dendrites in the transgenic population. The dendritic stem diameter correlates positively with the dendritic surface area and volume in both groups, but the total size of dendritic tree is greater at equivalent stem diameter in transgenic neurons.

These examinations suggest that enhanced dendritic growth triggered by permanent p21Ras activity results in proportional, correlative development of basal dendrites. However, alterations of the apical dendrites as a total are less proportional and less correlative. The extension of apical dendrites in the transgenic population is rather independent of perikaryal size, so that morphometric correlations such as those present in the wild type disappear. Because the apical dendrite is a more complex arborized structure combined of several modules (trunk, oblique dendrites, apical tuft), it is argued that their modifications might be differently affected owing to cortical lamination or other extrinsic determinants.

In previous studies of the rat visual cortex, Larkman (1991a,b) demonstrated that the terminal segments of basal trees contributed to a very high proportion of the combined dendritic length. For this reason, he expected that the number of dendritic tips and, hence, the number

of terminal segments in a tree would be related to other metric parameters of dendritic morphology. According to Larkman (1991b), the number of tips and, hence, the number of terminal sections, are positively correlated with the surface area of basal as well as apical dendrites. This relationship is confirmed by the data of the present study. A more mature neuronal environment allows evidently less plasticity, which would probably force dendritic growth in any possible direction, and so lead to even more irregular patterns. Pyramidal neurons of the transgenic population, however, preserved the above-mentioned correlative attributes. It is suggested, therefore, that these correlations may represent very conservative design principles of dendritic morphology, which cannot be affected significantly by artificial p21Ras activation in the phase of final differentiation or maintenance of cortical neurons.

A crucial aspect concerns the morphogenetic period during which the described morphological alterations become manifest in the transgenic animals. As mentioned above, p21Ras expression starts postnatally at about day 15, when neurons are postmitotic. Previous studies in rats showed that, although morphological differentiation of pyramidal neurons is not complete until the fourth postnatal week, the main developmental changes occur during the first 2 weeks after birth. The cell body of layer V pyramidal neurons reaches its adult size by the end of the second week, those of layer II/III pyramidal neurons 3 days later (Miller, 1981). The dendritic tree attains its mature appearance by the beginning of the third postnatal week,

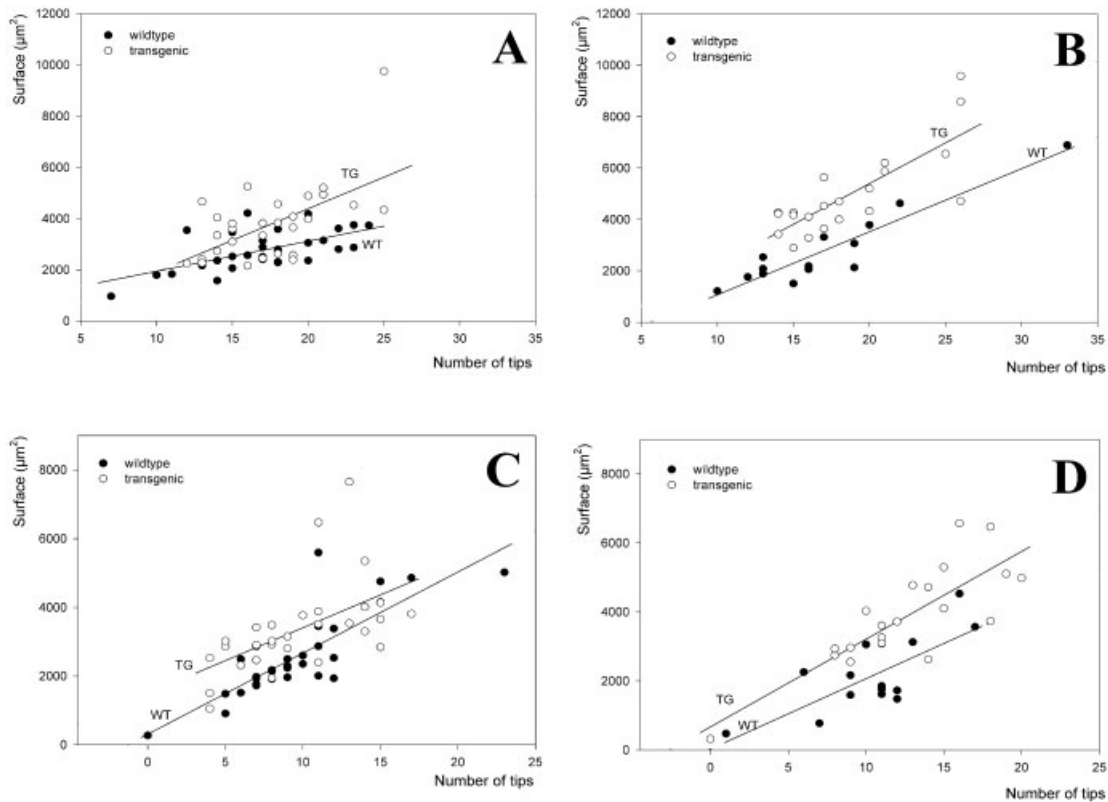


Fig. 10. Correlations between number of tips and surface area of the dendritic trees. **A:** Layers II/III, basal dendrites (TG:  $r = 0.57$ ,  $P = 0.001$ ; WT:  $r = 0.62$ ,  $P = 0.0003$ ). **B:** Layer V, basal dendrites (TG:  $r = 0.79$ ,  $P = 0.001$ ; WT:  $r = 0.93$ ,  $P < 0.0001$ ). **C:** Layers II/III, apical dendrites (TG:  $r = 0.56$ ,  $P = 0.0012$ ; WT:  $r = 0.81$ ,  $P < 0.0001$ ). **D:** Layer V, apical dendrites (TG:  $r = 0.82$ ,  $P < 0.0001$ ; WT:  $r = 0.75$ ,  $P = 0.002$ ).

when growth cones have almost completely disappeared (Wise et al., 1979; Juraska, 1982; Miller, 1981). The extension and complexity of the dendritic tree have been reported to increase significantly during the first 3 postnatal weeks, and by week 3 the dendritic arbor is nearly finished (Eayrs and Goodhead, 1959; Juraska and Fifkova, 1979; Wise et al., 1979; Miller, 1981).

Members of the Ras superfamily of G proteins have been shown to be very involved in the regulation of dendritic branch dynamics of neurons that have a relatively mature and established dendritic tree (Nakayama et al., 2000). During the late developmental phase of hippocampal pyramidal cells, RhoA is implicated in limiting the growth of dendrites by the retraction of existing branches (Nakayama et al., 2000). The reduction of the dendritic tree during the second postnatal week has earlier been reported using Golgi impregnation (Miller, 1981) and has been interpreted to result from the elimination of segments that were unable to establish sufficient synaptic support. This suggestion confirms recent findings that neuronal and synaptic activity guides dendritic development through mechanisms involving glutamate receptors and Rho GTPase-dependent modulation of the actin cytoskeleton (Li et al., 2002; Sin et al., 2002). Recently, also the p21Ras-dependent mitogen-activated protein kinase (MAPK) cascade has been reported to control dendritic morphogenesis by enhancing filopodial growth in activity-dependent neural development, and with the same mech-

anism it supports activity-dependent synapse clustering (Wu et al., 2001). Additionally, there is evidence that, during late postnatal and adult life, neurotrophins continue to act via *trk* receptors (Merlio et al., 1992; Fryer et al., 1996; Yan et al., 1997; Hayashi et al., 2000), which are known to trigger the intracellular p21Ras pathway.

Recent advances have revealed that short-term dendritic remodeling, i.e., extension and retraction of growth cones or processes, is accomplished by Rho GTPases-dependent rearrangement of the actin cytoskeleton and mainly is confined to dendritic tips and fine branches (Li et al., 2000; McAllister, 2000; Sin et al., 2002). Although some morphogenetic effects of p21Ras might be transduced by the activation of Rac and Cdc42 (Katoh et al., 2000; Negishi and Katoh, 2002), the present findings suggest a different mechanism that induces more profound and long-term morphological changes. Thus, constitutively active p21Ras increases the number of higher dendritic orders and even induces the formation of additional distal processes, but the major effect is the enlargement of proximal and intermediate segments. Insofar as the expression of p21H-ras<sup>Val12</sup> results in enhanced MAPK activity in this transgenic model (Holzer, 2001a), the particular changes in dendritic morphology might be mediated by MAPK-dependent pathways.

The observed morphological alterations in the p21H-ras<sup>Val12</sup> transgenic mice neocortex are due to effects within the late developmental phase and/or to effects that

proceed during adulthood. Although the late developmental phase is a preferred period for refining dendritic arbor, rapid dendritic changes and remodeling are also induced by activity-dependent TrkB activation in adult animals (Aloyz et al., 1999). Under both conditions, however, significant changes in the dendritic arbor are established after neuronal growth and main developmental maturation have been basically completed. Therefore, p21Ras might play an important role in plastic changes not only in early development but also during the final differentiation and maintenance of neurons.

## ACKNOWLEDGMENTS

We are grateful to Prof. Rolf Heumann and Dr. Hartmut Berns for providing the p21H-ras<sup>Val12</sup> transgenic mice for our experiments. The authors thank Prof. Johannes Seeger, head of the Department of Veterinary Anatomy, Leipzig, for allowing us to use the NeuroLucida system. Special gratitude is expressed for Dr. Johannes Kacza for his useful and continuous help. We also thank Jeroen Hoozemans for editorial advice and for critically reviewing the article.

## LITERATURE CITED

- Ahn NG. 1993. The MAP kinase cascade. Discovery of a new signal transduction pathway. *Mol Cell Biochem* 127/128:201–209.
- Aloyz R, Fawcett JP, Kaplan DR, Murphy RA, Miller FD. 1999. Activity-dependent activation of TrkB neurotrophin receptors in the adult CNS. *Learn Mem* 6:216–231.
- Baker RE, Dijkhuizen PA, Van Pelt J, Verhaagen J. 1998. Growth of pyramidal, but nonpyramidal, dendrites in long-term organotypic explants of neonatal rat neocortex chronically exposed to neurotrophin-3. *Eur J Neurosci* 10:1037–1044.
- Banker GA, Cowan WM. 1979. Further observations on hippocampal neurons in dispersed cell culture. *J Comp Neurol* 187:469–493.
- Bar-Sagi D, Feramisco JR. 1985. Microinjection of the Ras oncogene protein into PC12 cells induces morphological differentiation. *Cell* 42:841–848.
- Bartlett WP, Banker GA. 1984. An electron microscopic study of the development of axons and dendrites by hippocampal neurons in culture. I. Cells which develop without intercellular contacts. *J Neurosci* 4:1944–1953.
- Braitenberg V. 1978. Cortical architectonics: general and areal. In: Brazier MAB, Petsche H, editors. *Architectonics of the cerebral cortex*. New York: Raven Press. p 9–29.
- Brambilla R, Gnesutta N, Minichiello L, White G, Roylance AJ, Herron CE, Ramsey M, Wolfer DP, Cestari V, Rossi-Arnaud C. 1997. A role for the Ras signalling pathway in synaptic transmission and long-term memory. *Nature* 390:281–286.
- Bray D. 1973. Branching patterns of individual sympathetic neurons in culture. *J Cell Biol* 56:702–712.
- Colonnier M. 1968. Synaptic patterns on different cell types in the different laminae of the cat visual cortex. An electron microscope study. *Brain Res* 9:268–287.
- Davies AM. 2000. Neurotrophins: neurotrophic modulation of neurite growth. *Curr Biol* 10:R198–R200.
- Diamond J, Gray EG, Yasargil GM. 1970. The function of the dendritic spine: an hypothesis. In: Anderson P, Jansen JKS, editors. *Excitatory synaptic mechanisms*. Oslo: Universitetsforlaget. p 213–222.
- Duan H, Wearne SL, Morrison JH, Hof PR. 2002. Quantitative analysis of the dendritic morphology of corticocortical projection neurons in the macaque monkey association cortex. *Neuroscience* 114:349–359.
- Eayrs JT, Goodhead B. 1959. Postnatal development of the cerebral cortex of the rat. *J Anat* 93:385–402.
- Elston GN, Rockland KS. 2002. The pyramidal cell of the sensorimotor cortex of the macaque monkey: phenotypic variation. *Cereb Cortex* 12:1071–1078.
- Feldman ML. 1975. Serial thin sections of pyramidal apical dendrites in the cerebral cortex: spine topography and related observations. *Anat Rec* 181:354–355.
- Feldman ML. 1984. Morphology of the neocortical pyramidal neuron. In: Peters A, Jones EG, editors. *Cerebral cortex, vol 1: cellular components of the cerebral cortex*. New York: Plenum Press. p 123–200.
- Feldman ML, Dowd C. 1975. Loss of dendritic spines in aging cerebral cortex. *Z Anat Entwicklungsgesch* 148:279–301.
- Franklin KBJ, Paxinos G. 1997. *The mouse brain in stereotaxic coordinates*. New York: Academic Press.
- Fryer RH, Kaplan DR, Feinstein SC, Radeke MJ, Grayson DR, Kromer LF. 1996. Developmental and mature expression of full-length and truncated TrkB receptors in the rat forebrain. *J Comp Neurol* 374:21–40.
- Furth ME, Aldrich TH, Cordon-Cardo C. 1987. Expression of Ras proto-oncogene proteins in normal human tissues. *Oncogene* 1:47–58.
- Gärtner U, Holzer M, Arendt T. 1995. Induction of p21Ras in Alzheimer pathology. *Neuroreport* 6:1313–1316.
- Gärtner U, Holzer M, Arendt T. 1999. Elevated expression of p21Ras is an early event in Alzheimer's disease and precedes neurofibrillary degeneration. *Neuroscience* 91:1–5.
- Guerrero I, Wong H, Pellicier A, Burstein DE. 1986. Activated N-Ras gene induces neuronal differentiation of PC12 rat pheochromocytoma cells. *J Cell Physiol* 129:71–76.
- Hausser M, Spruston N, Stuart GJ. 2000. Diversity and dynamics of dendritic signaling. *Science* 290:739–744.
- Hayashi M, Mitsunaga F, Itoh M, Shimizu K, Yamashita A. 2000. Development of full-length Trk B-immunoreactive structures in the prefrontal and visual cortices of the macaque monkey. *Anat Embryol* 201:139–147.
- Heumann R. 1994. Neurotrophin signalling. *Curr Opin Neurobiol* 4:668–679.
- Heumann R, Narz F, Algür Y, Bartsch D, Hüser M, Klinz FJ, Wagner E, Berns H, Obst K, Wahle P. 1996. Neuronal modulation of p21Ras activity in transgenic animals: a master switch? *J Brain Res* 37:585.
- Heumann R, Goemans Ch, Bartsch D, Lingenhöhl K, Waldmeier PC, Hengeler B, Allegrini PR, Schellander K, Wagner EF, Arendt T, Kamdem RH, Obst-Pernberg K, Narz F, Wahle P, Berns H. 2000. Constitutive activation of Ras in neurons promotes hypertrophy and protects from lesion-induced degeneration. *J Cell Biol* 151:1537–1548.
- Holzer M, Gärtner U, Klinz FJ, Narz F, Heumann R, Arendt T. 2001a. Activation of mitogen-activated protein kinase cascade and phosphorylation of cytoskeletal proteins after neurone-specific activation of p21Ras. I. Mitogen-activated protein kinase cascade. *Neuroscience* 105:1031–1040.
- Holzer M, Rödel L, Seeger G, Gärtner U, Narz F, Janke C, Heumann R, Arendt T. 2001b. Activation of mitogen-activated protein kinase cascade and phosphorylation of cytoskeletal proteins after neurone-specific activation of p21Ras. II. Cytoskeletal proteins and dendritic morphology. *Neuroscience* 105:1041–1054.
- Horch HW, Katz LC. 2002. BDNF release from single cells elicits local dendritic growth in nearby neurons. *Nat Neurosci* 5:1177–1184.
- Horch HW, Kruttgen A, Portbury SD, Katz LC. 1999. Destabilization of cortical dendrites and spines by BDNF. *Neuron* 23:353–364.
- Huang EJ, Reichardt LF. 2001. Neurotrophins: roles in neuronal development and function. *Annu Rev Neurosci* 24:677–736.
- Huang EJ, Reichardt LF. 2003. TRK receptors: roles in neuronal signal transduction. *Annu Rev Biochem* 72:609–642.
- Jacobs B, Driscoll L, Schall M. 1997. Life-span dendritic and spine changes in areas 10 and 18 of human cortex: a quantitative Golgi study. *J Comp Neurol* 386:661–680.
- Jacobs B, Schall M, Prather M, Kapler E, Driscoll L, Baca S, Jacobs J, Ford K, Wainwright M, Treml M. 2001. Regional dendritic and spine variation in human cerebral cortex: a quantitative Golgi study. *Cereb Cortex* 11:558–571.
- Juraska JM. 1982. The development of pyramidal neurons after eye opening in the visual cortex of hooded rats: a quantitative study. *J Comp Neurol* 212:208–213.
- Juraska JM, Fikova E. 1979. A Golgi study of the early postnatal development of the visual cortex of the hooded rat. *J Comp Neurol* 183:247–256.
- Katoh H, Yasui H, Yamaguchi Y, Aoki J, Fujia H, Mori K, Negishi M. 2000. Small GTPase RhoG is a key regulator for neurite outgrowth in PC12 cells. *Mol Cell Biol* 20:7378–7387.
- Kleim JA, Swain RA, Czerlanis CM, Kelly JL, Pipitone MA, Greenough WT. 1997. Learning-dependent dendritic hypertrophy of cerebellar stellate cells: plasticity of local circuits. *Neurobiol Learn Mem* 67:29–33.
- Kolb B, Cote S, Ribeiro-da-Silva A, Cuello AC. 1997a. Nerve growth factor

- treatment prevents dendritic atrophy and promotes recovery of function after cortical injury. *Neuroscience* 76:1139–1151.
- Kolb B, Gorny G, Cote S, Ribeiro-da-Silva A, Cuello AC. 1997b. Nerve growth factor stimulates growth of cortical pyramidal neurons in young adult rats. *Brain Res* 751:289–294.
- Larkman AU. 1991a. Dendritic morphology of pyramidal neurons of the visual cortex of the rat: I. Branching patterns. *J Comp Neurol* 306:307–319.
- Larkman AU. 1991b. Dendritic morphology of pyramidal neurons of the visual cortex of the rat: II. Parameter correlations. *J Comp Neurol* 306:320–331.
- Li Z, Van Aelst L, Cline HT. 2000. Rho GTPases regulate distinct aspects of dendritic arbor growth in *Xenopus* central neurons in vivo. *Nat Neurosci* 3:217–225.
- Li Z, Aizenman CD, Cline HT. 2002. Regulation of the rho GTPases by crosstalk and neuronal activity in vivo. *Neuron* 33:741–750.
- Luo L, Jan LY, Jan YN. 1997. Rho family GTP-binding proteins in growth cone signalling. *Curr Opin Neurobiol* 7:81–86.
- McAllister AK. 2000. Cellular and molecular mechanisms of dendrite growth. *Cereb Cortex* 10:963–973.
- McAllister AK. 2002. Neurotrophins and cortical development. *Results Probl Cell Differ* 39:89–112.
- McAllister AK, Lo DC, Katz LC. 1995. Neurotrophins regulate dendritic growth in developing visual cortex. *Neuron* 15:791–803.
- McAllister AK, Katz LC, Lo DC. 1996. Neurotrophin regulation of cortical dendritic growth requires activity. *Neuron* 17:1057–1064.
- McAllister AK, Katz LC, Lo DC. 1997. Opposing roles for endogenous BDNF and NT-3 in regulating cortical dendritic growth. *Neuron* 18:767–778.
- Merlio JP, Ernfors P, Jaber M, Persson H. 1992. Molecular cloning of rat trkC and distribution of cells expressing messenger RNAs for members of the trk family in the rat central nervous system. *Neuroscience* 51:513–532.
- Mervis RF, Pope D, Lewis R, Dvorak RM, Williams LR. 1991. Exogenous nerve growth factor reverses age-related structural changes in neocortical neurons in the aging rat. A quantitative Golgi study. *Ann N Y Acad Sci* 640:95–101.
- Meyer G, Feldman EL. 2002. Signaling mechanisms that regulate actin-based motility processes in the nervous system. *J Neurochem* 83:490–503.
- Miller M. 1981. Maturation of rat visual cortex. I. A quantitative study of Golgi impregnated pyramidal neurons. *J Neurocytol* 10:859–878.
- Moore BD, Slopis JM, Jackson EF, De Winter AE, Leeds NE. 2000. Brain volume in children with neurofibromatosis type 1: relation to neuropsychological status. *Neurology* 54:914–920.
- Müller LJ, Verwer RW, Nunes Cardozo B, Vrensens G. 1984. Synaptic characteristics of identified pyramidal and multipolar nonpyramidal neurons in the visual cortex of young and adult rabbits. A quantitative Golgi-electron microscope study. *Neuroscience* 12:1071–1087.
- Nakayama AY, Harms MB, Luo L. 2000. Small GTPases Rac and Rho in the maintenance of dendritic spines and branches in hippocampal pyramidal neurons. *J Neurosci* 20:5329–5338.
- Negishi M, Katoh H. 2002. Rho family GTPases as key regulators for neuronal network formation. *J Biochem* 132:157–166.
- Niblock MM, Brunso-Bectold JK, Riddle DR. 2000. Insulin-like growth factor I stimulates dendritic growth in primary somatosensory cortex. *J Neurosci* 20:4165–4176.
- Nishida E, Gotoh Y. 1993. The MAP kinase cascade is essential for the diverse signal transduction pathways. *Trends Biochem Sci* 18:128–131.
- Noda M, Ko M, Ogura A, Liu DG, Amano T, Takano T, Ikawa Y. 1985. Sarcoma viruses carrying Ras oncogenes induce differentiation-associated properties in a neural cell line. *Nature* 318:73–75.
- Phillips LL, Belardo ET. 1994. Increase of c-fos and Ras oncoproteins in the denervated neuropil of the rat dentate gyrus. *Neuroscience* 58:503–514.
- Plaschke M, Souphanthong M, Wenzel J. 1995. Morphological alterations of hippocampal pyramidal neurons heterotopically transplanted into the somatosensory cortex of adult rats: a quantitative Golgi study. *Anat Embryol* 192:351–361.
- Rakic P. 1975. Role of cell interactions in development of dendritic patterns. *Adv Neurol* 12:117–134.
- Ramón y Cajal S. 1955. *Histologie du système nerveux de l'homme et des vertébrés*, vol II [Azoulay L, trans]. Madrid: Instituto Ramón y Cajal.
- Redmond L, Ghosh A. 2001. The role of Notch and Rho GTPase signaling in the control of dendritic development. *Curr Opin Neurobiol* 11:111–117.
- Ruchhoeft ML, Ohnuma S, McNeill L, Holt CE, Harris WA. 1999. The neuronal architecture of *Xenopus* retinal ganglion cells is sculpted by rho-family GTPases in vivo. *J Neurosci* 19:8454–8463.
- Scott EK, Luo L. 2001. How do dendrites take their shape? *Nat Neurosci* 4:359–365.
- Silva AJ, Frankland PW, Marowitz Z, Friedman E, Lazlo G, Cioffi D, Jacks T, Bourtschuladze R. 1997. A mouse model for the learning and memory deficits associated with neurofibromatosis type I. *Nat Genet* 15:281–284.
- Sin WC, Haas K, Ruthazer ES, Cline HT. 2002. Dendrite growth increased by visual activity requires NMDA receptor and Rho GTPases. *Nature* 419:475–480.
- Smith SJ. 1999. Dissecting dendrite dynamics. *Science* 283:1860–1861.
- Soloway AS, Pucak ML, Melchitzky DS, Lewis DA. 2002. Dendritic morphology of callosal and ipsilateral projection neurons in monkey prefrontal cortex. *Neuroscience* 109:461–471.
- Tanaka T, Ida N, Shimoda H, Waki C, Salamon D, Cline MJ. 1986. Organ specific expression of Ras oncoproteins during growth and development of the rat. *Mol Cell Biochem* 70:97–104.
- Thoenen H. 1995. Neurotrophins and neuronal plasticity. *Science* 270:593–598.
- Vaughn JE. 1989. Fine structure of synaptogenesis in the vertebrate central nervous system. *Synapse* 3:255–285.
- Whitford KL, Dijkhuizen P, Polleux F, Ghosh A. 2002. Molecular control of cortical dendrite development. *Annu Rev Neurosci* 25:127–149.
- Wise SP, Fleshmna JW Jr, Jones EG. 1979. Maturation of pyramidal cell form in relation to developing afferent and efferent connections of rat somatic sensory cortex. *Neuroscience* 4:1275–1297.
- Wong RO, Ghosh A. 2002. Activity-dependent regulation of dendritic growth and patterning. *Nat Rev Neurosci* 3:803–812.
- Wu GY, Deisseroth K, Tsien RW. 2001. Spaced stimuli stabilize MAPK pathway activation and its effects on dendritic morphology. *Nat Neurosci* 4:151–158.
- Yan Q, Radeke MJ, Matheson CR, Talvenheimo J, Welcher AA, Feinstein SC. 1997. Immunocytochemical localization of TrkB in the central nervous system of the adult rat. *J Comp Neurol* 378:135–157.